HHS Public Access

Author manuscript

J Chromatogr A. Author manuscript; available in PMC 2023 May 25.

Published in final edited form as:

J Chromatogr A. 2022 June 21; 1673: 463083. doi:10.1016/j.chroma.2022.463083.

Integration of a micropreconcentrator with solid-phase microextraction for analysis of trace volatile organic compounds by gas chromatography-mass spectrometry

Sujoy Halder[a], **Zhenzhen Xie**[a], **Michael H. Nantz**[b], **Xiao-An Fu**[a,*]

[a]Department of Chemical Engineering

[b]Department of Chemistry, University of Louisville, Louisville, KY 40208, United States

Abstract

The analysis of toxic volatile organic compounds (VOCs) in environmental air is important because toxic VOCs induce adverse effects on human health. Although gas chromatography- mass spectrometry (GC–MS) is the standard instrument for analysis of trace VOCs in air, this mode of analysis requires preconcentration and cryogenic processes. The preconcentration and subsequent thermal desorption of VOCs require special instruments and a long time of processing sample that significantly limit applications of GC–MS for monitoring indoor and outdoor VOC levels. Using a microfabricated preconcentrator for VOC analysis also has the challenge of a large sample volume for concentration. Using solid-phase microextraction (SPME) for VOC analysis by GC–MS often approaches the limit of detection of the GC–MS instrument for trace VOCs in air. This work reports a simple method to integrate microfabricated preconcentrators with commercial SPME fibers in a two-stage concentration processes to achieve rapid and reliable measurement of trace VOCs in air by GC–MS. We designed and fabricated a preconcentrator with micropillars in a microfluidic chamber to support sorbents and to increase the heat transfer rate to the sorbents for rapid thermal desorption. The effects of air flow rates through the preconcentrator on VOCs adsorption and thermal desorption were optimized for increasing analytical accuracy of VOCs measurements. The integration of a micropreconcentrator with SPME enabled measurements of sub-ppb levels of benzene, toluene, ethylbenzene, and xylene (BTEX), and trichloroethylene (TCE) in environmental air by GC–MS.

Keywords

VOCs; Micropreconcentrator; SPME; Two step preconcentration; GC–MS

*Corresponding author. xiaoan.fu@louisville.edu (X.-A. Fu).

CRediT authorship contribution statement

SH performed design and fabrication of the μPC devices and the experiments and data analysis and drafted the manuscript.
ZX performed the experiments and GC-MS analysis
MHN provided advice and reviewed the manuscript and obtained the funding.
XF provided guidance of design of the devices and experiments, data analysis and prepared the manuscript.

Declaration of Competing Interest

The authors declare no competing interest for this work.

Supplementary materials

Supplementary material associated with this article can be found, in the online version, at doi: 10.1016/j.chroma.2022.463083.

1. Introduction

The analysis of toxic volatile organic compounds (VOCs) in environmental air is important because toxic VOCs induce adverse effects on human health including cancers and cardiovascular diseases [1,2]. Among the wide spectra of VOC pollutants, significant attention has been given to benzene, toluene, ethylbenzene, and xylene (BTEX) and trichloroethylene (TCE) not only because of their toxicity and/or carcinogenic nature for chronic exposure, but also for their involvement in atmospheric photochemical reactions [3-5]. BTEX exposure has been responsible for numerous health conditions, such as skin and eye irritation, headache, neurological dysfunctions, and cardiovascular disease [1,3,6,7]. The sources of BTEX in environmental air include industrial emissions, automobile exhaust, petroleum products, and solvent usage [8-11]. Indoor BTEX sources are mostly cleaning products, paints, adhesives, cooking oil fumes, and vapor intrusion [4,12]. The US Occupational Safety and Health Administration (OSHA) set a short-term exposure limit of 5 ppm of BTEX over 15 min as a Permissible Exposure Limit (PEL) [13]. Trichloroethylene (TCE) harms the central nervous system, liver, kidney, immune and reproductive systems [14]. Chronic exposure to toxic BTEX at concentrations below their PEL causes cardiovascular disease and cancers [1-4]. Thus, there is still a need to develop convenient, rapid, and accurate analytical methods for periodically monitoring toxic VOCs in both indoor and outdoor air and to alert people and prevent their exposure to high levels of these VOCs.

Gas chromatography-mass spectrometry (GC–MS) is the golden standard tool for analysis of trace VOCs in environmental air, but this approach requires a long preconcentration time and large volumes of air samples [15]. The GC–MS method requires a special instrument for preconcentration and thermal desorption of VOCs. Simultaneous on-site quantification of VOCs in both indoor and outdoor air demands a highly sensitive instrument for lower concentration VOCs [16]. Several types of sensors including electromechanical sensor, metal oxide sensor, electronic nose, and gold nanoparticle-based sensor array, have been developed for detecting target VOCs in air [17]. Some of these techniques provide high sensitivity and lower detection limits toward target compounds, less power consumption, accurate and repeatable results; however, these sensors suffer significant interference by other VOCs in the air matrix [2].

Solid-phase microextraction (SPME) is a widely used sampling technique that uses polymer coated fibers to extract analytes from gas or liquid samples through adsorption. The quantity of analytes extracted by the SPME fiber depends on adsorption of VOCs on polymer coating material and is proportional to the analyte concentration [18-21]. The solventless SPME technique provides a linear response over an extensive range of analytes concentrations. SPME has been widely used for determination of VOCs in environmental air [15,18-20]; however, the analysis of sub-ppb levels of VOCs in air by SPME in conjunction with GC–MS is challenging because the limit of detection (LoD) of the instrument is approached at these levels [21-26].

Many miniaturized preconcentration and detection systems have been developed for portable analysis of toxic VOCs in environmental air. These include small-diameter tube and

needle extraction, SPME, and microfabricated preconcentrators. Most of the reported preconcentrators are fabricated using micro-electromechanical system (MEMS) technology to reduce the volume of the sorbent. These micropreconcentrators (μPC) have been primarily used as integral parts of micro-gas chromatograph (μGC) systems for field detection [27-31] or monitoring target VOCs in environmental air [32-35]. Micropreconcentrators can be loaded with different adsorbent materials to tailor affinities for target VOCs. Furthermore, μPCs can enhance the LoD and also improve selectivity by reducing interfering compounds or filtering undesirable compounds from a sample matrix [36]. In a recent publication, a μPC was mounted on unmanned aerial vehicle to collect and concentrate VOCs in air at different altitudes for subsequent analysis by GC–MS [37].

Although both microfabricated μPC and SPME methods have been used for analysis of VOCs in indoor and outdoor air, there is no study in which these two methods have been combined for analysis of trace VOCs by GC–MS. Both methods face challenges for accurate analysis of sub-ppb level VOCs in air by GC–MS because of the constraints of the detection limits of GC–MS for using SPME and large sample volume for using μPC. In this study, a MEMS-fabricated μPC was integrated with SPME to create a two-stage concentration process for analysis of BTEX and TCE in environmental air by GC–MS. Integration of these methods provides the advantages of smaller sample volume (less than a two-liter sample is required) for preconcentrator and avoiding sample dilution on thermal desorption by SPME. The microfluidic channel of the μPC device was filled with Carboxen 1000 to selectively trap gaseous BTEX and TCE. The adsorbed VOCs then were thermally desorbed to a small volume for extraction by SPME. This two-stage preconcentration method provides higher amounts of VOCs for GC–MS analysis than using either a μPC or SPME alone. The performance of the μPC device was characterized based on adsorption and desorption flow rates, recovery percentage, and thermal desorption efficiency. The two-stage preconcentration method was also examined for real-time measurements of BTEX and TCE in environmental air.

2. Material and methods

2.1. Chemicals and materials

Benzene, toluene, ethylbenzene, xylene (a mixture of *o*-, *m*-, and *p*-xylene), and TCE (analytical standard purity) were purchased from Sigma Aldrich. Tedlar bags, SPME holders and fibers coated with Carboxen/polydimethylsiloxane (Car/PDMS) (75 μm) coating, and Carboxen 1000 adsorbent were obtained from SUPELCO. Tedlar bags were cleaned by filling with synthetic air and then evacuating, and repeating the process three times. All chemicals used in this work were analytical grade and were used without further purification. Initially, a mixture of 41.6 μmol/m^3 BTEX and TCE was prepared by injecting predetermined amounts of the chemicals into a Tedlar bag containing 1×10^{-3} m^3 synthetic air. A serial dilution of this mixture was performed to achieve target concentrations for making calibration curves using SPME for extraction and GC–MS for analysis. Air-tight glass syringes were purchased from RESTEK. Freshly prepared standards were used for each experiment. Synthetic air (moisture < 0.16 μmol/m^3) was purchased from a local company (Welders Supply, Louisville, KY).

2.2. MEMS preconcentrator fabrication procedure

Micropreconcentrator devices (Fig. 1) with dimensions 14 mm x 8.5 mm x 1 mm, were designed and fabricated on a 10.16 cm diameter double-sided polished silicon wafer in the clean room of the Micro/Nano Technology Center at the University of Louisville. Two photomasks were prepared for the fabrication of the μPCs, the first was used to pattern the topside cavity and flow channel and the second was used for fabricating the backside microheater. The silicon wafer was cleaned and dried with acetone, methanol, DI water, and N_2, respectively, to remove any trace contaminants on the surface (Fig. 2A). The wafer then was placed in a furnace to form a ~400 nm thick SiO_2 layer (Fig. 2B). Wet thermal oxidation was run for 1.5 h at 1273.15 K. The silicon oxide layer thickness was measured using a filmetrics system and determined to be 430 nm. A positive photoresist Shipley 1827 was coated on both sides of the oxidized wafer followed by soft bake at 363.15 K for 2 min. One side of the wafer was then exposed to UV light (Karl Suss Mask Aligner MA6/BA6, hard contact) through a dark field photomask. The wafer was developed in Microposit MF319 solution for 90 s, rinsed under a DI water bath, and then dried using a stream of N_2 (Fig. 2C). The wafer was examined under an optical microscope to check the patterns and defects before hard-baking for 2 min using a hotplate at 393.15 K. The silicon oxide layer was patterned by etching with buffered oxide etchant (BOE) to expose silicon areas for deep reactive ion etching (DRIE) (Fig. 2D). DRIE was used to create a central cavity and flow channels consisting of a set of micropillars having a diameter of 150 μm spaced 100 μm apart near the inlet and outlet sections to retain adsorbents. Another set of micropillars with a diameter of 100 μm spaced 650 μm apart was created inside the cavity to promote rapid heat transfer from an on-board heater to the adsorbent particles. An additional flow channel was formed on the side of the cavity for loading adsorbents inside the chamber of the sealed device (Fig. 2E). Its depth was measured as 400 μm using the Dektek profilometer. The wafer then was immersed in a *N*-methyl-2-pyrrolidone bath at 333.15 K to strip the photoresist and followed by oxygen plasma cleaning for 10 min to completely remove photoresist residues. Sacrificial SiO_2 layers were completely removed by placing the wafer in a BOE solution for 5 min (Fig. 2F). After BOE treatment, the wafer was washed in a DI water bath and dried under a N_2 flow. The wafer was sealed by anodic bonding to a glass wafer (Pyrex 7740 glass, 500 μm thick) using a Suss SB6e bonder (Fig. 2G). The backside of the glass-bonded wafer was coated with a Shipley 1827 photoresist and patterned to form a microheater using backside alignment. Photolithography was performed similarly. Image reversal was done to alternate the action of the photoresist. This process improves the profile for the lift-off step by providing higher resolution, re-entrant sidewalls. The wafer was then subjected to ammonia exposure at 363.15 K and followed by flood exposure (Karl Suss Mask Aligner MA6/BA6) for 25 s, which made the photoresist in the UV-unexposed area soluble to the developer solvent. After development, the wafer was hard-baked for 2 min at 403.15 K (Fig. 2H). The wafer was sputtered (Kurt J. Lesker PVD 75) with chromium (Cr) and tungsten (W) metals for 2 min and 35 min, respectively (Fig. 2I). Before metal sputtering, the wafer surface was cleaned with O_2 plasma (March RIE CS1701) to remove any organics for better adhesion of the metals to the wafer. The metal on the photoresist was removed by the lift-off process using acetone to dissolve the photoresist (Fig. 2J). A 550 nm-thick metal layer (Cr layer ~30 nm and W layer ~520 nm) was deposited as a microheater and resistance temperature detector (RTD). The wafer was finally diced to

afford the individual μPC devices. The inlets and outlets of the μPCs were connected with deactivated silica tubes (355 μm O.D., 255 μm I.D., Polymicro Technologies) and secured with silicone adhesive (Duraseal®*1531, Cotronics, NY USA). Carboxen 1000 adsorbent (4.5 ± 0.1 mg, surface area 1200 m^2/g) was loaded into the μPC with the assistance of an applied vacuum. After filling with adsorbent, the port for loading the adsorbent was sealed with Duraseal 1531. The volume filled by the adsorbent was around 1×10^{-8} m^3. The packing density was 450 kg/m^3.

2.3. Standard sample preparation and calibration curves

The amounts of individual compounds of BTEX and TCE measured by GC–MS were calculated based on individual calibration curves. Different concentrations of standard analytes ranging from 41.6 $nmol/m^3$ to 2.08 $\mu mol/m^3$ were prepared and transferred to a 50 cm^3 air-tight glass syringe. A Car/PDMS SPME fiber was inserted into the glass syringe for a 15 min sampling time and then manually inserted into the GC–MS injection port for analysis. The 15 min sampling time was maintained for each concentration. The SPME fiber was thermally desorbed for cleaning before sampling and confirmed as VOC-free by the absence of any signals by GC–MS. Analyte peaks were well separated and less peak broadening was noticed. The xylene isomer sample showed two peaks corresponding to *m*-/*p*-xylene and *o*-xylene isomers, respectively and the peak area ratio of *m*-/*p*-xylene to *o*-xylene was about 4:1. The total xylene peak area was counted by combining the areas of the *m*-/*p*-xylene and *o*-xylene peaks. A calibration curve was obtained by plotting the peak area from GC–MS response versus concentration for each analyte (Figure S1 in Supplementary Material). The coefficient of determination (R^2) is higher than 0.99 for all analytes as shown in Table 1. The slopes of calibration lines are significantly different among the analytes because of differences in molecular weight of the analytes and interaction between SPME surface coating and individual analytes.

2.4. LoD, LoQ of GC–MS with SPME sampling

The LoD and limit of quantification (LoQ) for the SPME process were calculated from the calibration curves using a linear regression model. LoD = 3.3*(Sy/S) and LoQ = 10*(Sy/S), where Sy is the standard deviation of the response and S is the slope of the calibration curve. Sy is acquired by multiplying the square root of sample numbers with a standard error obtained from regression analysis. The calibration equations, LoD, and LoQ are presented in Table 1 for all analytes. The LoD of all compounds were a few $\mu g/m^3$. Because concentrations of BTEX and TCE in environmental air are at the levels of these LoD and LoQ when using SPME in conjunction with GC–MS, there is a need to increase the analyte concentrations in order to increase the amounts extracted by SPME for accurate quantitative analysis.

2.5. Analytical procedure

Fig. 3 shows a schematic of the experimental setup for integration of μPC and SPME as a two stage preconcentration process. The overall process of analyzing standard BTEX and TCE samples includes four steps. The first step is to preconcentrate VOC analytes using the μPC. The μPC device was heated and flowed with synthetic air at 593.15 K for 20 min to remove contaminants. A mixture of 41.6 $nmol/m^3$ of each BTEX analyte and

TCE was prepared from a 41.6 μmol/m^3 sample by dilution with synthetic air. Different volumes of this mixture then were passed through the conditioned μPC where the analytes were adsorbed on adsorbent at room temperature. Adsorption was examined at different sample flow rates (20, 30, 40, 50 cm^3/minute) and an optimized flow rate was selected. The second step is the thermal desorption process of VOCs from the μPC. The μPC was placed on a preheated hotplate. The top surface of the μPC reached 593.15 K within 1 min. For these experiments, the microheater on the micropreconcentrator was not used due to high resistance and maximum temperature of about 423.15 K. A thermometer (Omega, model hh806au) with a K-type thermocouple was used to measure the temperature on the surface of the μPC. When the temperature reached 593.15 K, synthetic air from the cylinder was passed through the μPC at an optimized flow rate of 40 cm^3/min. The first 50 cm^3 of the desorbed sample was collected in a clean glass syringe. The third step is to utilize SPME extraction from the desorbed sample. The SPME fiber was conditioned before extraction to remove any background contaminants. The SPME fiber (Car/PDMS) then was inserted into the glass syringe with a short silicon rubber tube with a septum (RESTEK Septa Thermolite® Shimadzu Plug) for sealing for an optimized time (15 min) to adsorb the analytes at room temperature. The last step is to analyze compounds from the SPME by GC–MS. The SPME fiber was immediately transferred to the injection port of the GC. Thermal desorption of the analytes from the SPME fiber was carried out in a split injection mode of 5:1 for the GC at 573.15 K for 1.5 min.

2.6. GC–MS parameters

Analyses were performed using a GC–MS (Agilent 7820A GC system, 5975 Series MSD) equipped with an HP-1 column (30 m × 0.25 mm id, 0.25 μm thickness). GC oven temperature was programmed to 313.15 K, 3-min hold, then ramped to 393.15 K at a rate of 10 K/min following a 1-min hold. Helium was used as the carrier gas with a flow rate of 1 cm^3/min using the split injection mode. The injection port temperature was set at 573.15 K.

3. Results and discussion

3.1. Characterization of the preconcentrator–SPME approach for analysis of VOCs

The performance of a μPC is determined by a number of variables including the device structure, types of adsorbents, adsorbent capacity, porosity, selectivity, power consumption, flow dynamics, and pressure drop across the device [38]. A preconcentration factor (PF) has been used to evaluate the performance of a μPC. There is no standard definition of PF as researchers have used different criteria to calculate it. In general, PF is the ratio of the concentration of analytes after thermal desorption to the initial concentration of a gas sample [39]. Since the concentration of analytes after a preconcentration process depends on the initial sample volume and sampling conditions including sample flow rate and time, the PF depends on these variables. Alfeeli *et al.* defined PF as the ratio between peak areas generated by the detector (FID) with/without the μPC [40]. Tian *et al.* used the ratio of volume in which gas is occupied initially to the volume after thermal desorption [41]. McCartney *et al.* used a correlation with flow rate and sampling time of adsorption and desorption to calculate PF [36]. In this study, we used recovery percentage (%) of target analytes to measure the device performance instead of PF. The recovery percentage was

determined by $(C_x \times V_x)/(C_i \times V_i) \times 100\%$, where C_x and V_x were the analyte concentration and volume after thermal desorption. C_i and V_i were initial analyte concentration and volume before concentration process by the μPC.

To determine recovery percentages, different concentrations (20.8, 41.6, 83.2, and 124.8 nmol/m^3) of BTEX and TCE in 5×10^{-3} m^3 synthetic air were passed through the device. The adsorption flow rate was set to 50 cm^3/min. The captured analytes then were collected by thermal desorption directly into a 50 cm^3 air-tight syringe. The desorption flow rate and temperature were fixed at 50 cm^3/min and 593.15 K, respectively. The optimization of desorption temperature and the flow rates for adsorption and desorption are discussed in later sections. The concentrations of the collected samples were measured after a SPME concentration process and analysis by GC–MS using calibration curves. The SPME extraction time was fixed at 15 min based on the literature [19-22] and our experimental data of optimized extraction time in Figure S2 in the Supplementary Material. Fig. 4 represents the calculated recoveries for different analyte concentrations at a fixed sample volume of 5×10^{-3} m^3. The average recoveries were 99.6%, 98.8%, 69.6%, 66.5%, and 81.2% for benzene, toluene, ethylbenzene, xylene, and TCE, respectively. For benzene and toluene, high recovery percentages were achieved, which indicate that most of these compounds adsorbed in the μPC and then were collected after thermal desorption. Relatively lower values were observed for ethylbenzene, xylene, and TCE. One possible reason could be related to the adsorbent property as the trapping capacity can vary with different compounds based on volatility. Also, some residues might not be desorbed completely. Nevertheless, similar recovery percentage results were acquired by using different concentrations of these analytes. The relative standard deviation in recoveries for these four samples was lower than 8%, showing very good reproducibility for analysis. Furthermore, SPME was carried out for 15 min on two 50 cm^3 samples, one containing 41.6 nmol/m^3 and the other containing 1664 nmol/m^3 of BTEX compounds and TCE. The GC–MS chromatograms for these analyses are shown in Fig. 5. For comparison purpose, 41.6 nmol/m^3 of BTEX and TCE in 2×10^{-3} m^3 sample was passed through the μPC at a flow rate of 50 cm^3/min and then thermally desorbed at 593.15 K. The desorbed sample was collected in 50 cm^3 using a desorption flow rate of 40 cm^3/min. The desorbed sample was then extracted by SPME for 15 min and analyzed by GC–MS. Fig. 5 shows the signals of BTEX and TCE from preconcentrated 2×10^{-3} m^3 of 41.6 nmol/m^3 using a combination of the μPC and SPME. The results indicate that the μPC with carboxen adsorbent could concentrate 2×10^{-3} m^3 of 41.6 nmol/m^3 to 50 cm^3 of 1664 nmol/m^3 for benzene, TCE and toluene, but there was some loss of ethylene and xylene. According to SPME theory, the amounts of extracted analytes are proportional to the sample concentrations for the same SPME and sample volumes [25-26]. Thus, increasing sample concentration by the μPC is important for increasing the extracted amounts of analytes by SPME and consequently enhancing GC–MS signals. The results show the advantage of combining the μPC with SPME for two-stage concentration and extraction to significantly increase GC–MS detection signals for accurate measurements of trace VOCs.

3.2. The effect flow rates for adsorption/thermal desorption of the preconcentrator

The flow rates for adsorption and thermal desorption are important parameters to characterize the μPC device performance. Higher sample flow rate affects adsorption capacity. The packed adsorbent bed residence time is determined by the sample flow rate of adsorption process. When the residence time is shorter than the critical residence time, the adsorption capacity decreases and causes breakthrough earlier. The maximum flow rate achieved for the μPC was 50 cm^3/min using a KNF diaphragm vacuum pump. An optimized adsorption flow condition was determined using a range of adsorption flow rates (20 to 50 cm^3/min) for 166.4 nmol/m^3 of BTEX and TCE in 2×10^{-3} m^3. Desorption flow rate and temperature for this set of experiments were set at 40 cm^3/min and 593.15 K, respectively. After SPME, GC–MS chromatograms were obtained. There were no significant changes in recovery (%) for BTEX and TCE with increasing adsorption flow rate, as shown in Figure S3. The relative standard deviation (RSD,%) of recoveries for the above-mentioned flow ranges was lower than 5%. An optimum adsorption flow rate of 50 cm^3/min was chosen for the sample concentrations of BTEX and TCE less than 166.4 nmol/m^3 for further experiments.

The results in Figure S4 show the recoveries (%) at different desorption flow rates (10 to 40 cm^3/min) using 41.6 nmol/m^3 of BTEX and TCE in 5×10^{-3} m^3. A constant adsorption flow rate of 50 cm^3/min and desorption temperature of 593.15 K were maintained in this study. Desorbed analytes were collected to a volume of 50 cm^3 of desorbed air from the μPC. The results show that recoveries were lowest for the 10 cm^3/min desorption flow rate which indicates the lowest desorption efficiency. The recoveries were improved with higher flow rates of 20 to 40 cm^3/min. So, 40 cm^3/min was used in the desorption step for the next experiments. Also, another important observation was to check desorption efficiency by eluting all adsorbate inside the μPC using a long thermal desorption process. The collected second 50 cm^3 from thermal desorption was also analyzed. It yielded no detectable BTEX and TCE peaks. This result indicated that a collection of the first 50 cm^3 is sufficient to extract all adsorbed analytes from the μPC.

3.3. The effect of thermal desorption temperature of the preconcentrators

Desorption temperature is another important parameter that influences μPC performance. Heat is applied to the device to increase the temperature to rapidly release any adsorbed analytes. However, increasing temperature above certain levels can cause decomposition of captured analytes, which results in inaccurate sensing for analytes in the detection step. In this study, detector responses were measured at different desorption temperatures (473.15 K, 523.15 K, 553.15 K, 593.15 K and 633.15 K) with fixed preconcentration conditions (initial BTEX and TCE concentration of 83.2 nmol/m^3, sample volume of 2×10^{-3} m^3, adsorption and desorption flow rates at 50 cm^3/min and 40 cm^3/min, respectively, and a thermally desorbed sample volume of 50 cm^3). The desorption step started by keeping the μPC device on a preheated hotplate and heated to gain a desired temperature. Within 1 min the temperature of the device reached the desired point. The temperature on the top surface of the device was measured by a K-type thermocouple. Then synthetic air was flowed at 40 cm^3/min and collected to a glass syringe. SPME and GC–MS analysis was performed to measure the analytes. Fig. 6 shows the values of recoveries as a function of

desorption temperature. The effect of desorption temperature on the recovery is obvious for all compounds. At 473.15 K, low recoveries were observed for all analytes, indicating incomplete desorption of these analytes. Recoveries increased with higher temperatures; benzene and TCE reached maximum recovery at 553.15 K. Similarly, toluene, ethylbenzene and xylene recoveries increased with temperature up to 593.15 K. Recoveries were observed to decrease at 633.15 K desorption temperature. The recommended desorption temperature for the Carboxen-1000 adsorbent is 523.15 K. Increasing the temperature beyond this temperature can cause decomposition of analytes to result in lower recovery. So, 593.15 K was chosen for the desorption step to produce reliable and repeatable results for analysis of environmental air samples.

3.4. Analysis of environmental air samples using the micropreconcentrator with SPME

The reproducibility of different devices was tested to ensure reliable results in the long term. To evaluate reproducibility, three different μPC devices were used to analyze 5×10^{-3} m^3 of 83.2 nmol/m^3 BTEX and TCE samples using the same experimental conditions of adsorption flow rate: 50 cm^3/min, desorption flow rate: 40 cm^3/min, desorption temperature of 593.15 K, desorbed volume of 50 cm^3 for SPME extraction. These three devices yielded nearly identical peak areas (RSD < 10%) for all target analytes which indicate the repeatability among different devices. Furthermore, 2×10^{-3} m^3 of 41.6 nmol/m^3 and 1×10^{-3} m^3 of 83.2 nmol/m^3 BTEX and TCE gaseous samples were analyzed using the two-stage preconcentration process with the same μPC devices and SPME. The peak areas for all analytes were very close as shown in the supporting Figure S5. Therefore, these devices are reliable for reproducible results.

After the verification of the reproducibility of the integrated two stage preconcentration process with the same μPC devices and SPME, this approach was applied to detect BTEX and TCE in environmental air. Air samples of 1×10^{-3} m^3 were collected from a gas station near an exit of interstate highway and a city roadside in Louisville, Kentucky at different times using cleaned Tedlar bags. Three air samples were taken from each location and each air sample was processed with different μPCs. The samples flowed through the μPC at a flow rate of 50 cm^3/min, then thermally desorbed at 593.15 K using synthetic air as the carrier gas with a flow rate of 40 cm^3/min. The desorbed samples were collected to a volume of 50 cm^3 and then SPME was performed for 15 min. The SPME fiber was desorbed into the GC injection port and analyzed by GC–MS. Table 2 shows the results obtained from a gas station near an interstate highway and a city roadside at two different times. All compound concentrations are in the ranges of the same compounds collected with passive sampling devices over each two-week period for one year in Louisville, Kentucky in a recent publication [5]. The GC–MS chromatograms for the roadside is given as an example in Fig. 7. Air samples with only SPME extraction were also tested by GC–MS for comparison and very tiny peaks were detected. The results show the advantage of integration of the μPC and SPME for increasing the GC–MS signals for quantitative analysis.

Toluene was found as the most abundant compound of BTEX in environmental air. The mean levels of benzene and toluene were higher during the afternoon rush hours than in the morning as their source was principally car exhaust. The total mean concentration of

BTEX and TCE near the gas station during rush hour was 1.731 μg/m^3, while the total mean concentration of these compounds at the roadside during rush hour was 1.886 μg/m^3. Other unknown peaks were obtained with different retention times, but because this work focused on method development and analysis of BTEX and TCE, these compounds are presently unidentified.

4. Conclusion

In this study, a MEMS preconcentrator was developed to integrate with SPME to significantly increase the amounts of extracted analytes for GC–MS analyses which in turn enables reliable measurements of VOCs at a few μg/m^3 levels in environmental air. The performance of the μPC was characterized based on the optimized operation parameters of adsorption and thermal desorption for BTEX and TCE gaseous mixtures, which are toxic pollutants in environmental air. Reproducible measurements were demonstrated with different μPCs and SPME. The optimized method has been applied to analyze trace BTEX and TCE in environmental air samples.

Supplementary Material

Refer to Web version on PubMed Central for supplementary material.

Acknowledgement

This work was supported by funding from NIH (P42 ES023716).

References

[1]. Kampa M, Castanas E, Human health effects of air pollution, Environ Pollut 151 (2008) 362–367, doi:10.1016/j.envpol.2007.06.012. [PubMed: 17646040]

[2]. Allouch A, Le Calvé S, Serra CA, Portable, miniature, fast and high sensitive real-time analyzers: BTEX detection, Sens. Actuators B Chem 182 (2013) 446–452, doi:10.1016/j.snb.2013.03.010.

[3]. Miri M, Shendi MRA, Ghaffari HR, Aval HE, Ahmadi E, Taban E, Gholizadeh A, Aval MY, Mohammadi A, Azari A, Investigation of outdoor BTEX: concentration, variations, sources, spatial distribution, and risk assessment, Chemosphere 163 (2016) 601–609, doi:10.1016/j.chemosphere.2016.07.088. [PubMed: 27589149]

[4]. Lara-Lbeas I, Rodríguez-Cuevas A, Andrikopoulou C, Person V, Baldas L, Colin S, Le Calvé S, Sub-ppb level detection of BTEX gaseous mixtures with a compact prototype GC equipped with a preconcentration unit, Micromachines (Basel) 10 (2019) 187, doi:10.3390/mi10030187. [PubMed: 30871284]

[5]. Mukerjee S, Smith LA, Thoma EB, Whitaker DA, Oliver KD, Duvall R, Cousett AT, Spatial analysis of volatile organic compounds using passive samplers in the Rubbertown industrial area of Louisville, Kentucky, USA, Atmos. Pollut. Res 11 (2020) 81–86, doi:10.1016/j.apr.2020.02.021. [PubMed: 32699520]

[6]. Hazrati S, Rostami R, Farjaminezhad M, Fazlzadeh M, Preliminary assessment of BTEX concentrations in indoor air of residential buildings and atmospheric ambient air in Ardabil, Iran, Atmos. Environ 132 (2016) 91–97, doi:10.1016/j.atmosenv.2016.02.042.

[7]. Na K, Moon K-C, Kim YP, Source contribution to aromatic VOC concentration and ozone formation potential in the atmosphere of Seoul, Atmos. Environ 39 (2005) 5517–5524, doi:10.1016/j.atmosenv.2005.06.005.

[8]. Hoque RR, Khillare P, Agarwal T, Shridhar V, Balachandran S, Spatial and temporal variation of BTEX in the urban atmosphere of Delhi, India, Sci Total Environ 392 (2008) 30–40, doi:10.1016/j.scitotenv.2007.08.036. [PubMed: 18067950]

[9]. Zalel A, Broday Yuval DM, Revealing source signatures in ambient BTEX concentrations, Environ Pollut 156 (2008) 553–562, doi:10.1016/j.envpol.2008.01.016. [PubMed: 18289752]

[10]. Yassaa N, Brancaleoni E, Frattoni M, Ciccioli P, Isomeric analysis of BTEXs in the atmosphere using β-cyclodextrin capillary chromatography coupled with thermal desorption and mass spectrometry, Chemosphere 63 (2006) 502–508, doi:10.1016/j.chemosphere.2005.08.010. [PubMed: 16364404]

[11]. Atkinson R, Atmospheric chemistry of VOCs and NOx, Atmos. Environ 34 (2000) 2063–2101, doi:10.1016/S1352-2310(99)00460-4.

[12]. Romagnoli P, Balducci C, Perilli M, Vichi F, Imperiali A, Cecinato A, Indoor air quality at life and work environments in Rome, Italy, Environ. Sci. Pollut. Res. Int 23 (2016) 3503–3516, doi:10.1007/s11356-015-5558-4. [PubMed: 26490929]

[13]. Lewis G, Continuous monitoring of benzene, toluene, ethyl benzene, and xylenes (BTEX) in air with the Thermo Scientific Sentinel PRO Environmental Mass Spectrometer, Thermo Fisher Scientific (2014) 0–4 https://tools.thermofisher.com/content/sfs/brochures/EPM-AppNote-Sentinel.pdf.

[14]. Chiu WA, Jinot J, Scott CS, Makris SL, Cooper GS, Dzubow RC, Bale AS, Evans MV, Guyton KZ, Keshava N, Human health effects of trichloroethylene: key findings and scientific issues, Environ. Health Perspect 121 (2013) 303–311, doi:10.1289/ehp.1205879. [PubMed: 23249866]

[15]. Tumbiolo S, Gal J-F, Maria P-C, Zerbinati O, Determination of benzene, toluene, ethylbenzene and xylenes in air by solid phase micro-extraction/gas chromatography/mass spectrometry, Anal. Bioanal. Chem 380 (2004) 824–830, doi:10.1007/s00216-004-2837-1. [PubMed: 15517200]

[16]. Namieśnik J, Zygmunt B, Jastrzębska A, Application of solid-phase microextraction for determination of organic vapours in gaseous matrices, J. Chromatogr. A 885 (2000) 405–418, doi:10.1016/s0021-9673(99)01157-7. [PubMed: 10941687]

[17]. Spinelle L, Gerboles M, Kok G, Persijn S, Sauerwald T, Review of portable and low-cost sensors for the ambient air monitoring of benzene and other volatile organic compounds, Sensors 17 (2017) 1520, doi:10.3390/s17071520. [PubMed: 28657595]

[18]. Koziel J, Jia M, Khaled A, Noah J, Pawliszyn J, Field air analysis with SPME device, Anal. Chim. Acta 400 (1999) 153–162, doi:10.1016/S0003-2670(99)00614-5.

[19]. Larroque V, Desauziers V, Mocho P, Development of a solid phase microextraction (SPME) method for the sampling of VOC traces in indoor air, J. Environ. Monit 8 (2006) 106–111, doi:10.1039/b511201j. [PubMed: 16395466]

[20]. Merkle S, Kleeberg KK, Fritsche J, Recent developments and applications of solid phase microextraction (SPME) in food and environmental analysis–A review, Chromatography 2 (2015) 293–381, doi:10.3390/chromatography2030293.

[21]. Baimatova N, Koziel JA, Kenessov B, Quantification of benzene, toluene, ethylbenzene and o-xylene in internal combustion engine exhaust with time-weighted average solid phase microextraction and gas chromatography mass spectrometry, Anal. Chim. Acta 873 (2015) 38–50, doi:10.1016/j.aca.2015.02.062. [PubMed: 25911428]

[22]. Baimatova N, Kenessov B, Koziel JA, Carlsen L, Bektassov M, Demyanenko OP, Simple and accurate quantification of BTEX in ambient air by SPME and GC–MS, Talanta 154 (2016) 46–52, doi:10.1016/j.talanta.2016.03.050. [PubMed: 27154647]

[23]. Riboni N, Trzcinski JW, Bianchi F, Massera C, Pinalli R, Sidisky L, Dalcanale E, Careri M, Conformationally blocked quinoxaline cavitand as solid-phase microextraction coating for the selective detection of BTEX in air, Anal. Chim. Acta 905 (2016) 79–84, doi:10.1016/j.aca.2015.12.005. [PubMed: 26755140]

[24]. Koziel JA, Pawliszyn J, Air sampling and analysis of volatile organic compounds with solid phase microextraction, J. Air Waste Manag. Assoc 51 (2001) 173–184, doi:10.1080/10473289.2001. [PubMed: 11256496]

[25]. Pawliszyn J, Theory of solid-phase microextraction, J. Chromatogr. Sci 38 (2000) 270–278. [PubMed: 10901412]

[26]. Ouyang G, Pawliszyn J, Recent developments in SPME for on-site analysis and monitoring, TrAC Trends Anal. Chem 25 (2006) 692–703, doi:10.1016/J.TRAC.2006.05.005.

[27]. Skog KM, Xiong F, Kawashima H, Doyle E, Soto R, Gentner DR, Compact, automated, inexpensive, and field-deployable vacuum-outlet gas chromatograph for trace-concentration gas-phase organic compounds, Anal. Chem 91 (2019) 1318–1327, doi:10.1021/acs.analchem.8b03095. [PubMed: 30605307]

[28]. Garg A, Akbar M, Vejerano E, Narayanan S, Nazhandali L, Marr LC, Agah M, Zebra GC, A mini gas chromatography system for trace-level determination of hazardous air pollutants, Sens. Actuators B Chem 212 (2015) 145–154, doi:10.1016/j.snb.2014.12.136.

[29]. Lewis PR, Manginell P, Adkins DR, Kottenstette RJ, Wheeler DR, Sokolowski SS, Trudell DE, Byrnes JE, Okandan M, Bauer JM, Recent advancements in the gas-phase MicroChemLab, IEEE Sens. J 6 (2006) 784–795, doi:10.1109/JSEN.2006.874495.

[30]. Sukaew T, Chang H, Serrano G, Zellers ET, Multi-stage preconcentrator/focuser module designed to enable trace level determinations of trichloroethylene in indoor air with a microfabricated gas chromatograph, Analyst 136 (2011) 1664–1674, doi:10.1039/c0an00780c. [PubMed: 21359357]

[31]. Bryant-Genevier J, Zellers ET, Toward a microfabricated preconcentrator-focuser for a wearable micro-scale gas chromatograph, J. Chromatogr. A 1422 (2015) 299–309, doi:10.1016/j.chroma.2015.10.045. [PubMed: 26530144]

[32]. Lahlou H, Vilanova X, Correig X, Gas phase micro-preconcentrators for benzene monitoring: a review, Sens. Actuators B Chem 176 (2013) 198–210, doi:10.1016/j.snb.2012.10.004.

[33]. Breuil P Camara EHM, Briand D, De Rooij NF, Pijolat C, A micro gas preconcentrator with improved performance for pollution monitoring and explosives detection, Anal. Chim. Acta 688 (2011) 175–182, doi:10.1016/j.aca.2010.12.039. [PubMed: 21334483]

[34]. Camara EHM, Breuil P, Briand D, Guillot L, Pijolat C, de Rooij NF, A Micro Gas Preconcentrator with improved performances for environmental monitoring, International Solid-State Sensors, Actuators and Microsystems Conference, IEEE (2009) 983–986, doi:10.1109/SENSOR.2009.5285982.

[35]. Zampolli S, Elmi I, Mancarella F, Betti P, Dalcanale E, Cardinali GC, Severi M, Real-time monitoring of sub-ppb concentrations of aromatic volatiles with a MEMS-enabled miniaturized gas-chromatograph, Sens. Actuators B Chem 141 (2009) 322–328, doi:10.1016/J.SNB.2009.06.021.

[36]. McCartney MM, Zrodnikov Y, Fung AG, LeVasseur MK, Pedersen JM, Zamuruyev KO, Aksenov AA, Kenyon NJ, Davis CE, An easy to manufacture micro gas preconcentrator for chemical sensing applications, ACS Sens 2 (2017) 1167–1174, doi:10.1021/acssensors.7b00289. [PubMed: 28753000]

[37]. Simms LA, Borras E, Chew BS, Matsui B, McCartney MM, Robinson SK, Kenyon N, Davis CE, Environmental sampling of volatile organic compounds during the 2018 Camp Fire in Northern California, J. Environ. Sci 103 (2021) 135–147.

[38]. Alfeeli B, Agah M, Toward handheld diagnostics of cancer biomarkers in breath: micro preconcentration of trace levels of volatiles in human breath, IEEE Sens. J 11 (2011) 2756–2762, doi:10.1109/JSEN.2011.2160390.

[39]. Lee J, Lee J, Lim S-H, Micro gas preconcentrator using metal organic frame-work embedded metal foam for detection of low-concentration volatile organic compounds, J. Hazard. Mater 392 (2020) 122145, doi:10.1016/j.jhazmat.2020.122145. [PubMed: 32070927]

[40]. Alfeeli B, Cho D, Ashraf-Khorassani M, Taylor LT, Agah M, MEMS-based multi-inlet/outlet preconcentrator coated by inkjet printing of polymer adsorbents, Sens. Actuators B Chem 133 (2008) 24–32, doi:10.1016/j.snb.2008.01.063.

[41]. Tian WC, Pang SW, Lu CJ, Zellers ET, Microfabricated preconcentrator-focuser for a microscale gas chromatograph, J. Microelectromech. Syst 12 (2003) 264–272, doi:10.1109/JMEMS.2003.811748.

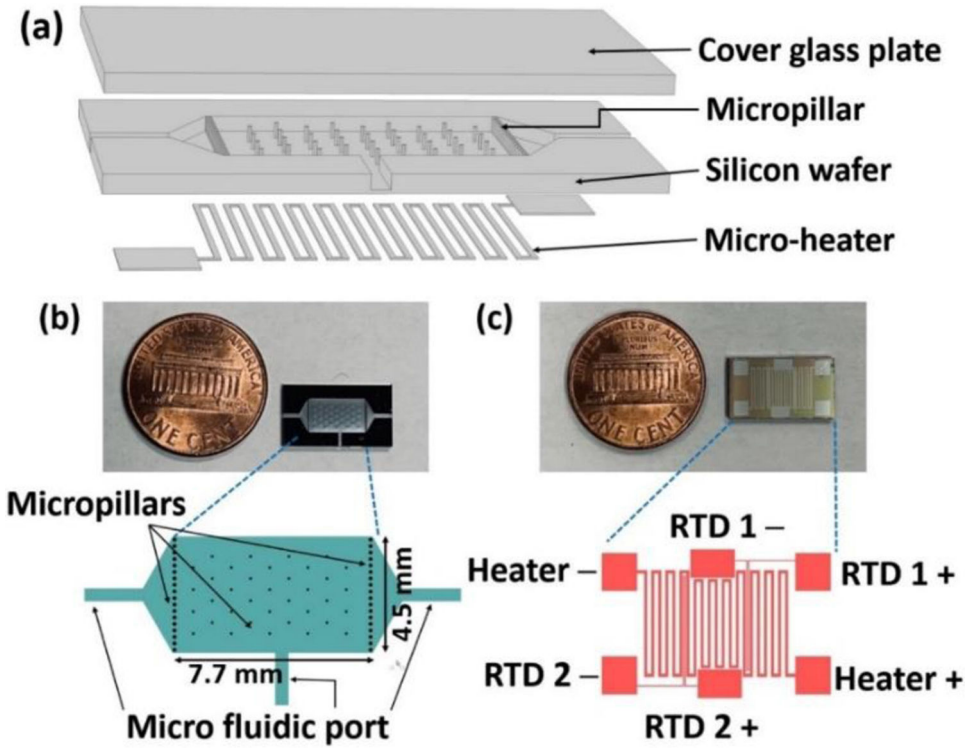

Fig. 1.

Micro gas preconcentrator (μPC): (a) three-dimensional view of layers; (b) image of front side of the μPC showing cavity and micropillars; and (c) image of backside heater and RTD of the μPC.

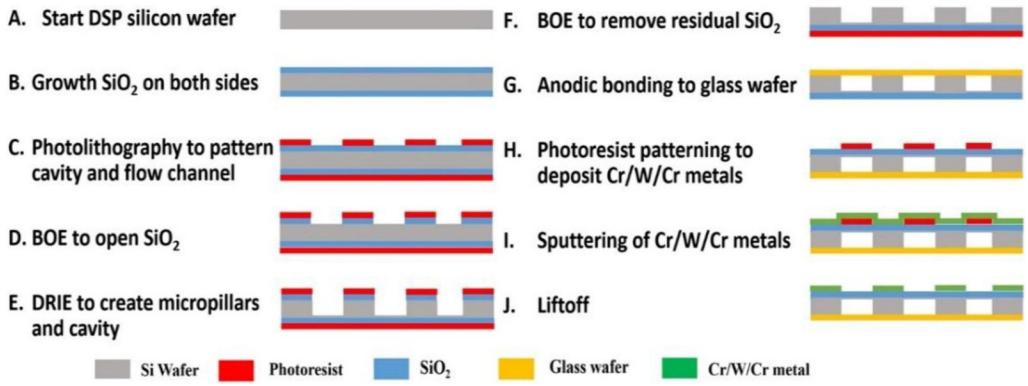

Fig. 2.
Schematic illustration of the μPC fabrication steps.

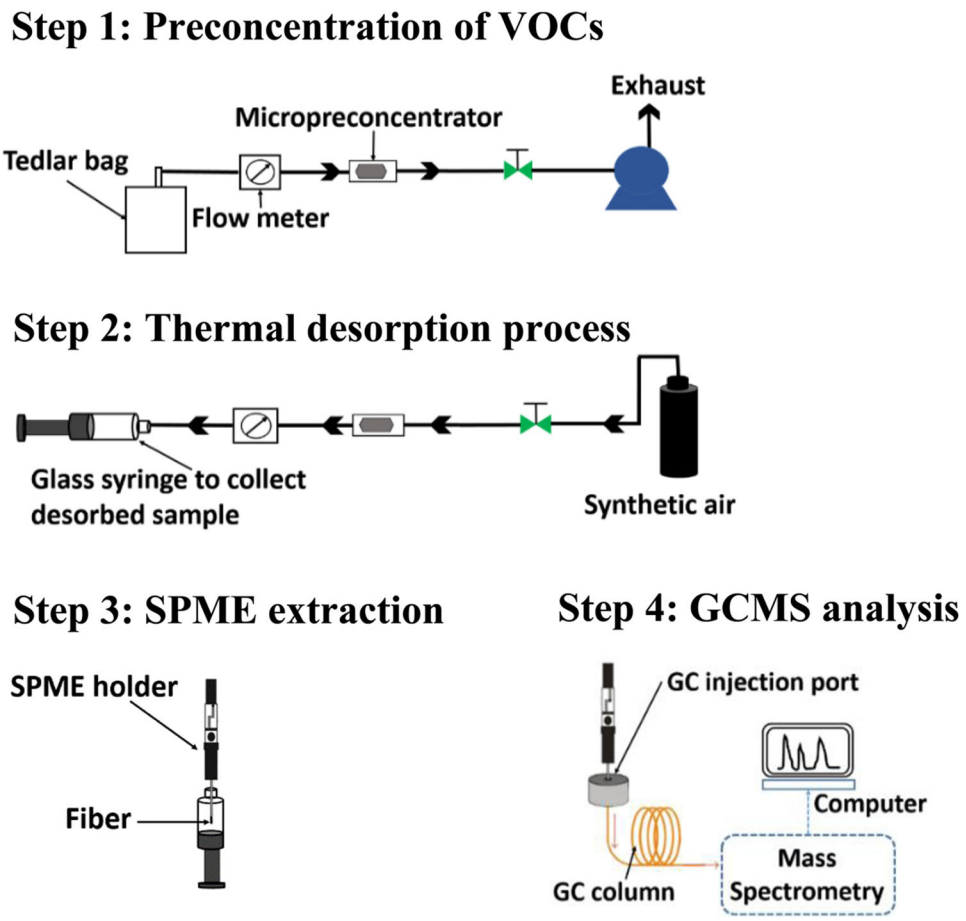

Fig. 3.
Scheme of the analytical procedure from adsorption of samples to GCMS analysis.

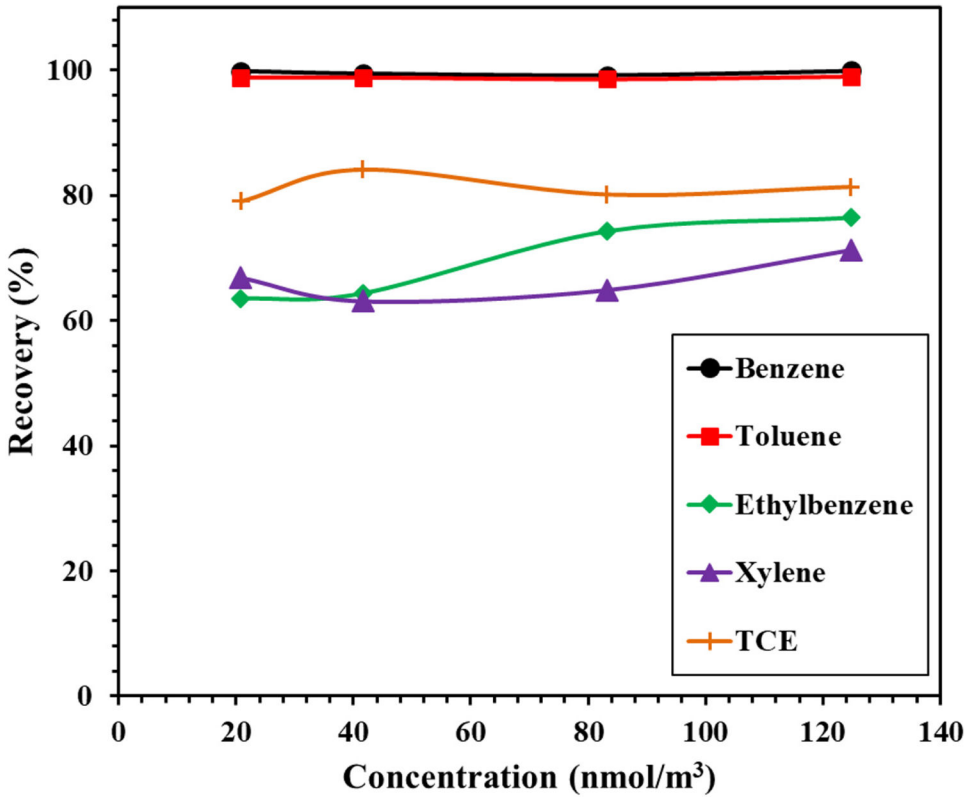

Fig. 4.

Recovery percentage of BTEX and TCE for a combination of μPC and SPME at different initial concentrations (20.8, 41.6, 83.2, and 124.8 nmol/m^3) in 5×10^{-3} m^3 samples.

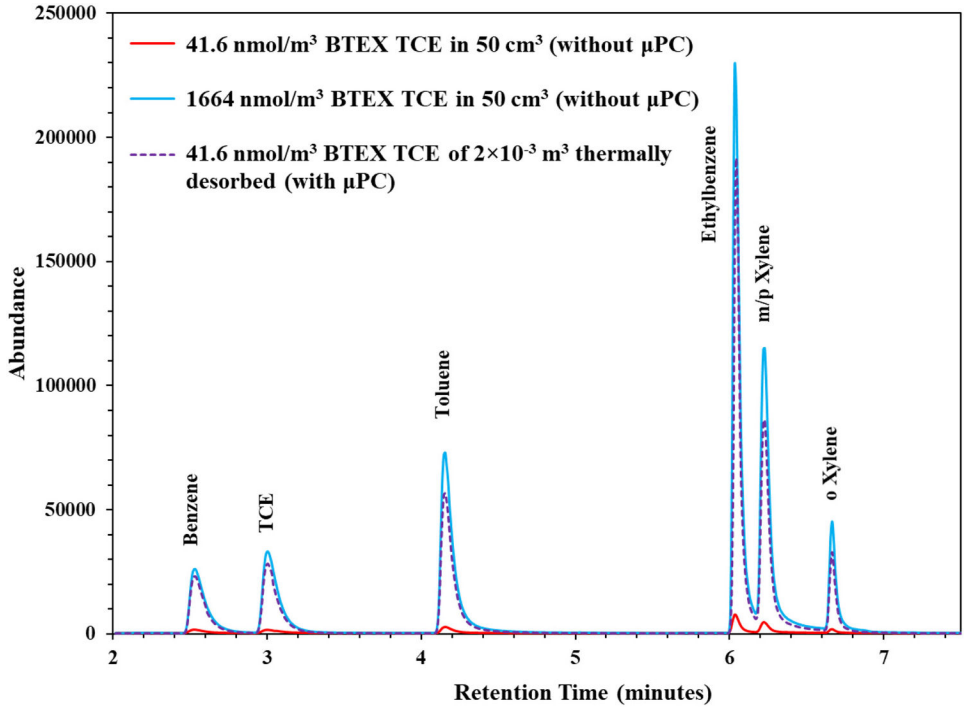

Fig. 5.

A comparison of detector signals for SPME of 41.6 nmol/m^3 and 1664 nmol/m^3 BTEX TCE of 50 cm^3 samples (without µPC) with 41.6 nmol/m^3 BTEX TCE of 2×10^{-3} m^3 concentrated by the µPC and then thermally desorbed to 50 cm^3 for SPME.

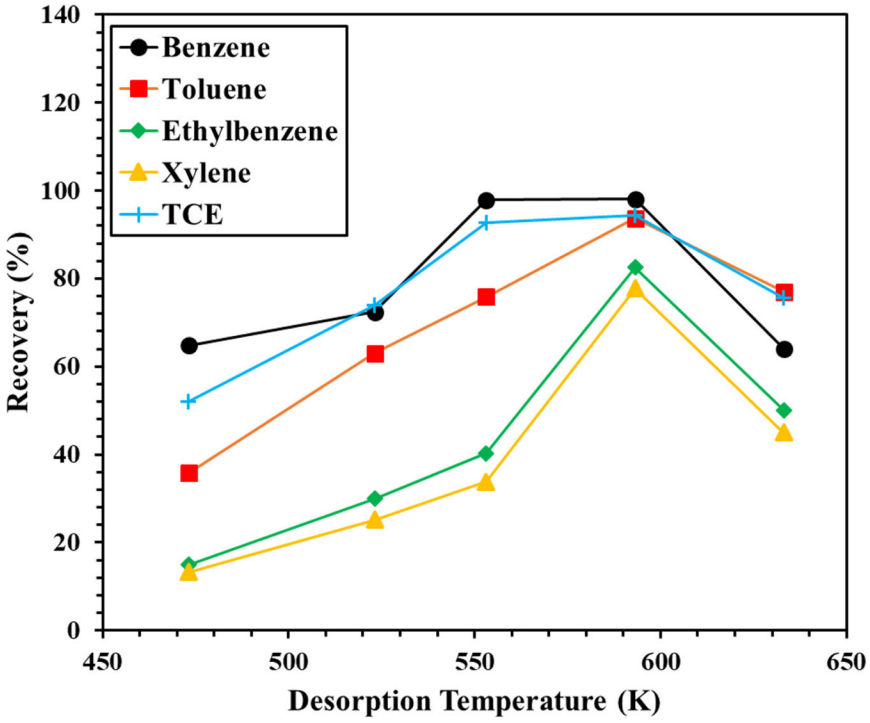

Fig. 6.

Recoveries obtained at different desorption temperature for 83.2 nmol/m^3 of 2×10^{-3} m^3 BTEX and TCE preconcentrated into 50 cm^3 samples.

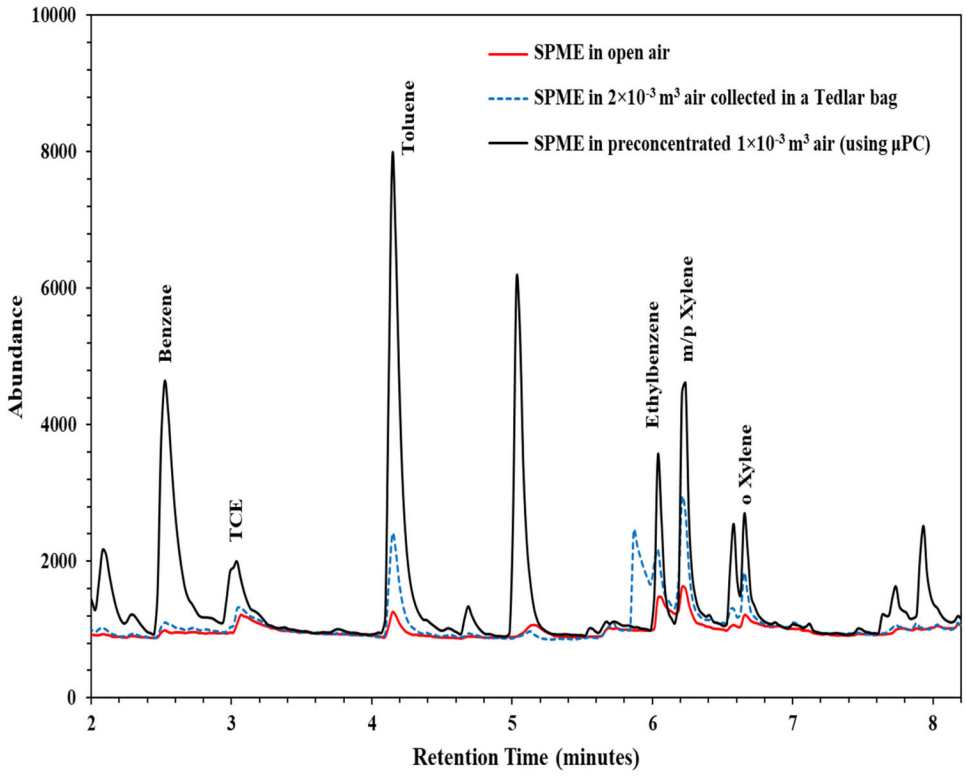

Fig. 7.

GC-MS spectra for environmental air sample; (a) red line: SPME for 15 min extraction in open air (b) blue dash line: SPME for 15 min extraction in 2 × $^{-3}$ m^3 air collected in a Tedlar bag (c) black line: SPME for 15 min extraction of 50 cm^3 sample preconcentrated from 1 × 10^{-3} m^3 air using the µPC.

Table 1

Calibration equations, LoD, and LoQ obtained for BTEX and TCE.[a].

Compound	Calibration equation	R^2	LoD (μg/m^3)	LoQ (μg/m^3)
Benzene	Y = 10,326 * X	0.9963	2.66	8.07
Toluene	Y = 19,690 * X	0.9966	2.46	7.46
Ethylbenzene	Y = 29,891 * X	0.9985	1.67	5.04
Xylene	Y = 23,349 * X	0.9957	2.88	8.72
TCE	Y = 7843.8 * X	0.9985	1.63	4.95

[a]Y and X correspond to the detector signal (peak area) and analyte concentration (μg/m3), respectively.

Table 2

Average concentrations (μg/m^3) and standard deviations (n = 3) of BTEX and TCE in ambient air with 1 × 10^{-3} m^3 samples preconcentrated by the μPC and SPME.

	Gas station(10 AM)	Gas station(5 PM)	Roadside(10 AM)	Roadside(5 PM)
Benzene	0.495 ± 0.019	0.48 ± 0.028	0.418 ± 0.026	0.483 ± 0.042
Toluene	1.162 ± 0.034	1.731 ± 0.138	1.667 ± 0.062	1.886 ± 0.164
Ethylbenzene	0.451 ± 0.033	0.55 ± 0.009	0.182 ± 0.005	0.599 ± 0.039
Xylene	0.576 ± 0.012	0.918 ± 0.003	0.417 ± 0.024	0.689 ± 0.048
TCE	0.303 ± 0.006	0.287 ± 0.001	0.322 ± 0.026	0.384 ± 0.011